Coulomb interactions and delocalization in quantum Hall constrictions

Leonid P. Pryadko
Institute for Advanced Study, Princeton, New Jersey 08540

Efrat Shimshoni
Department of Mathematics-Physics, Oranim–Haifa University, Tivon 36006, Israel

Assa Auerbach
Department of Physics, The Technion, Haifa 32000, Israel
(Received 29 October 1999)

We study a geometry-dependent effect of long-range Coulomb interactions on quantum Hall (QH) tunneling junctions. In an *X*-shaped geometry, duality relates junctions with opening angles α and $(\pi-\alpha)$. We prove that duality between weak tunneling and weak backscattering survives in the presence of long-range interactions, and that their effects are precisely cancelled in the self-dual geometry $\alpha=\pi/2$. Tunneling exponents as a function of α, the interaction strength χ, and the filling fraction ν are calculated. We find that Coulomb interaction induces localization in narrow channels (large α), and delocalization for sharply pinched constrictions (small α). Consequently, an insulator-to-metal transition happens at an angle $\alpha_c(\chi,\nu)\leqslant\pi/2$. We discuss the implications of our results for tunneling experiments in QH-constriction and cleaved-edge geometries.

I. INTRODUCTION

The idea of current-carrying edge states[1] is one of the major paradigms in the theory of the quantum Hall (QH) effect. For simple filling fractions $\nu=(2m+1)^{-1}$, Wen has shown[2–6] that edge modes can be represented as one-component chiral Luttinger liquids, with the universal coupling determined by ν. Within this simple model, controlled calculations are possible. This leads to many elegant results, including the universal interedge tunneling exponent,[5,7] exact expressions for tunneling conductance, the nonlinear tunneling *I-V* curve,[8,9] and tunneling noise.[10–12]

Experimentally, however, there are more dimensions to this problem. The results of the first pinch-off tunneling experiment,[13] where the scaling appeared to be in agreement with theory,[5,7] have only recently received a partial confirmation.[14,15] Furthermore, in Ref. 16 no scaling was observed at all, and in Ref. 17 the measured tunneling exponent was off by a factor of 2. Such discrepancies were attributed in part to edge reconstruction in samples with ''soft'' confinement.[18] However, the tunneling measurements in cleaved-edge samples,[19,20] where the confining potential is expected to be sharp, yield tunneling exponents shifted off the predicted values even at the magic filling fractions $\nu=1,\ 1/3$.

Previously, much effort[21] was dedicated to identify mechanisms leading to (nonuniversal) corrections to tunneling exponents. In particular, the effect of the long-range Coulomb interaction was analyzed[22–25] in the geometry of two counterpropagating parallel edges ($\alpha\to 0$ in Fig. 1). In exact analogy with its effect in a one-dimensional electron gas,[26] repulsive Coulomb interaction renormalizes the Luttinger liquid coupling parameter. Thus, a weak impurity-associated interedge tunneling becomes a relevant perturbation, so that the current flow (from top to bottom in Fig. 1) is *enhanced* at low temperature *T* and applied voltage *V*. However, the same interaction *suppresses*[25] the tunneling in the dual configuration, of two semi-infinite nonchiral Luttinger liquids connected by a tunneling point ($\alpha\to\pi$ in Fig. 1), and the system is pushed towards the insulating regime. This indicates that even the *sign* of the Coulomb interaction effect on the tunneling exponent is not the same in different geometries.

The purpose of this work is to analyze in detail the Coulomb interaction effect on the properties of QH tunneling junctions in different geometries. First, we demonstrate that the well-known duality relating weak tunneling and weak backscattering remains exact in the presence of long-range interactions. Then, we focus on scale-invariant *X*-shaped constrictions, and calculate the renormalized Luttinger coupling constant $g_\star^2$ (which, in particular, determines the power law dependence of the conductance on *T* and *V*) as a function of the opening angle α (Fig. 1). We show that the unscreened Coulomb interaction drives a zero-temperature delocalization transition as a function of α in both integer and fractional QH constrictions. In the integer case the transition occurs precisely at the self-dual value $\alpha_c=\pi/2$, independent of the interaction strength. At the fractions $\nu=(2m+1)^{-1}$, the critical angle α_c is nonuniversal, but its value is always smaller than $\pi/2$. We also analyze the effect of Coulomb

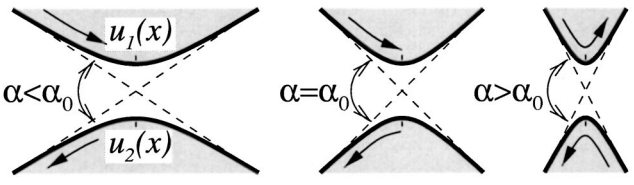

FIG. 1. Shading denotes quantum Hall regions bounded by counterpropagating edge modes u_1, u_2. In a saddle-point geometry, Coulomb interactions suppress the up-down tunneling for large opening angles α, and enhance it for small α. This effect cancels *exactly* in the self-dual geometry, $\alpha=\pi/2$.

 ©2000 The American Physical Society

interactions in the geometry of cleaved-edge tunneling experiments.

The paper is organized as follows. In Sec. II we introduce the tunneling action that accounts for the long-range interactions. A general proof of the duality between weak tunneling and weak backscattering is given in Sec. III. In Sec. IV, we present our results for the renormalized Luttinger coupling $g_\star^2$ in different geometries, and in Sec. V we discuss the implications on tunneling experiments. Related analytic results are collected in the Appendices: in Appendix A, the case of $\alpha=\pi$ is solved; in Appendix B, the Wiener-Hopf technique is used to directly solve the self-dual case $\alpha=\pi/2$, and evaluate the lowest-order correction for $|\cos\alpha|\ll 1$.

II. THE EFFECTIVE TUNNELING ACTION

Gapless edge excitations $u\equiv u(x,\tau)$ for Laughlin's QH states with filling fractions $\nu=(2m+1)^{-1}$ can be described[4–6] by the imaginary-time quadratic action

$$\mathcal{S}_0=\frac{1}{4\pi}\int_0^\beta d\tau\int dx\,\partial_x u(i\partial_\tau u+v\partial_x u), \tag{1}$$

where x is the coordinate along the edge, and $v\equiv v(x)$ is the edge wave velocity. The field u is related to the linear charge density at the edge, $\rho=\sqrt{\nu}\partial_x u/(2\pi)$ (note the unconventional normalization).

Formally, gauge invariance requires that the field $u(x,\tau)$ be treated as a compact boson of radius $R=\sqrt{\nu}$, i.e., the values u and $u+2\pi\sqrt{\nu}$ must be identified. This, however, is *not* achieved within the usual path integral formalism[27] in a finite geometry if we assume the field $u(x,\tau)$ continuous everywhere along the circumference. Indeed, the equal-time commutation relationship

$$[u(x),u(x')]=i\pi\,\mathrm{sgn}(x-x')$$

on the edge of length L implies that the fields $u_0\equiv u(0,\tau)$ and $u_L\equiv u(L,\tau)$ are canonically conjugated, which contradicts the continuity of the field along the circle. The difference u_L-u_0 (proportional to the topological charge associated with the zero mode) is also proportional to the total charge $Q=\sqrt{\nu}(u_L-u_0)/(2\pi)$ accumulated at the edge; only in the absence of tunneling into the edge this charge is a dynamically conserved quantized quantity. The correct zero-mode quantization spectrum can be obtained if we consider the variables u_0 and u_L as independent, and write the bare edge action (1) more explicitly as[28]

$$\mathcal{S}_0=\frac{1}{4\pi}\int_0^\beta d\tau\int_0^L dx\,\partial_x u(i\partial_\tau u+v\partial_x u)+\frac{1}{8\pi}\int_0^\beta d\tau(u_L-u_0)i\partial_\tau(u_L+u_0). \tag{2}$$

The boundary term in the second line is added to fix the canonical quantization of the zero mode, and to decouple it from the edge modes with finite momenta.[29]

Since the charge density ρ is expressed linearly in terms of the field u, the action remains quadratic[6,23,30] even in the presence of nonlocal Coulomb interaction

$$\mathcal{S}_1=\frac{\nu e^2}{8\pi^2\varepsilon}\int_0^\beta d\tau\int dx\,dy\,u'(x)V(|\mathbf{r}_x-\mathbf{r}_y|)u'(y), \tag{3}$$

where $\mathbf{r}_x$ is the actual position of the point x as measured along the edge, and ε is the dielectric constant of the material. The problem is nontrivial because now both the distance x measured along the edge, and the geometrical distance $|\mathbf{r}_x-\mathbf{r}_y|$ are important.

The interedge tunneling is introduced by the nonlinear term

$$\mathcal{S}_t=\int_0^\beta d\tau\,\mathrm{Re}\,\lambda e^{ig\varphi},\quad \varphi\equiv u(x_1)-u(x_2); \tag{4}$$

here $g=\sqrt{\nu}$ for the quasiparticles' tunneling between the points x_1 and x_2 through the QH liquid with the filling fraction ν, or $g\to\tilde{g}=1/\sqrt{\nu}$ for tunneling of electrons through the insulating region. The tunneling amplitude λ is set by the details[31] of the self-consistent potential near the tunneling point and considered as a phenomenological parameter.

The nonlinear tunneling action (4) depends on the values of the field $u(x,\tau)$ in the points x_1, x_2; the values of this field in all other points can be integrated out. Leaving the argument φ of the tunneling term as the only independent variable, we can write the most general form of the effective action

$$S=\frac{T}{4\pi}\sum_n|\omega_n|\mathcal{K}(\omega_n)|\varphi_n|^2+\int_0^\beta d\tau\,\mathrm{Re}\,\lambda e^{ig\varphi(\tau)}, \tag{5}$$

where the harmonics $\varphi_n\equiv\int_0^\beta d\tau\varphi(\tau)\exp(-i\omega_n\tau)$ and $\overline{\varphi_n}\equiv\varphi_{-n}$ are evaluated at the Matsubara frequencies $\omega_n=2\pi nT$. This effective tunneling model is fully characterized by the frequency-dependent coupling $\mathcal{K}(\omega_n)$, which contains all relevant information about the form of the interaction potential $V(r)$ and the geometry of the system. Formally, its functional form is defined by the correlator[28]

$$\mathcal{K}^{-1}(\omega_n)=\frac{|\omega_n|}{2\pi}\langle|\varphi_n|^2\rangle_{\lambda=0}. \tag{6}$$

If the coupling $\mathcal{K}(\omega)$ is independent of the frequency, the effective action (5) can be visualized as describing an overdamped particle in a periodic (cosine) potential with Ohmic dissipation $\kappa=\mathcal{K}/g^2$; the transport properties for this problem are known exactly.[8,9] In general, however, the exact solution is not available, and we have to rely on the frequency-shell perturbative renormalization group (RG). The main idea is that the nonlinear term is irrelevant for large-frequency modes $\varphi(\omega)$, as long as $|\omega|\gg\lambda$. When such modes are integrated out, the tunneling constant for the remaining slow modes is reduced,

$$\lambda(\Lambda)=\lambda(\Lambda_0)\langle e^{ig\varphi}\rangle_{\Lambda<\omega<\Lambda_0}, \tag{7}$$

or, equivalently,

$$-\ln\frac{\lambda(\Lambda)}{\lambda(\Lambda_0)}=g^2\int_{\Lambda_0}^{\Lambda}\frac{d\omega}{2\pi}\langle|\varphi(\omega)|^2\rangle_{\lambda=0}=g^2\int_{\Lambda_0}^{\Lambda}\frac{d\omega}{\omega\mathcal{K}(\omega)},$$

where we used the definition (6). After the frequencies are rescaled to restore the original upper cutoff, we arrive at the usual RG equation

$$\frac{d\ln\lambda}{d\ln\Lambda}=1-g^2\mathcal{K}^{-1}(\Lambda)\equiv 1-g_\star^2(\Lambda). \tag{8}$$

The renormalization stops at a lower cutoff scale determined either by the temperature or the applied voltage. Most importantly, for $g_\star^2>1$, the tunneling amplitude flows to weak coupling as the temperature is lowered, so that the channel along the tunneling current becomes more insulating; for $g_\star^2<1$ it flows to strong coupling.

It should be pointed out that in the case where $\mathcal{K}(\omega)$ is *frequency independent*, the parameter $g_\star^2$ [defined in Eq. (8)] is a constant, and the effective Euclidean action describing the system can be recast in the simpler form

$$S=\frac{T}{4\pi}\sum_n |\omega_n|\,|\varphi_n|^2+\int_0^\beta d\tau\,\mathrm{Re}\,\lambda e^{ig_\star\varphi(\tau)}. \tag{9}$$

Such is indeed the case (for sufficiently small ω) for the scale-invariant models considered in detail in Sec. IV. In this situation, the RG equation leads to the standard result[7,12]

$$\lambda_{\mathrm{eff}}\sim\max(T,V)^{g_\star^2-1}, \tag{10}$$

which can be also obtained by expanding the exact solution.[8,9]

III. DUALITY BETWEEN WEAK TUNNELING AND WEAK BACKSCATTERING

The partition function corresponding to the effective action (5) [which also describes an overdamped particle in a non-Ohmic dissipative environment, $\kappa(\omega)=\mathcal{K}(\omega)/g^2$] can be also rewritten[32,33] in terms of the dual variable $\Delta\theta$ with the identical action, up to a replacement $\mathcal{K}(\omega_n)\to 1/\mathcal{K}(\omega_n)$, $g\to 1/g$, and the modified tunneling coefficient $\lambda\to\tilde{\lambda}$ (which has the meaning of fugacity for the instanton of the original field φ). In terms of edge modes, this duality[9,8] represents a freedom to describe the same junction in terms of *weak* tunneling or *strong* backscattering, and vice versa. The main advantage of the duality is the ability to substitute a problem at *strong* tunneling with its dual, which can be then accessed perturbatively.

This argument relies heavily on the properties of the effective model (5), which, in principle, may or may not remain equivalent to the original edge model after the addition of the nonlocal coupling (3). To illustrate the mutual consistency of the two models, we derive the relationship between the coupling $\mathcal{K}(\omega)$ in the two tunneling geometries directly, using only the quadratic action $\mathcal{S}_q\equiv\mathcal{S}_0+\mathcal{S}_1$.

Consider a field configuration with the boundary conditions fixed as in Fig. 2(a), where $u_i=u_i(\tau)$ are given. Everywhere on the composite contour $C\equiv C_1+C_2$ the action is quadratic, and the corresponding Euler-Lagrange equation is linear,

$$\partial_x\left[i\partial_\tau u+v(x)\partial_x u+\frac{\nu e^2}{2\pi\varepsilon}\int_C dy\,V(|\mathbf{r}_x-\mathbf{r}_y|)\partial_y u\right]=0.$$

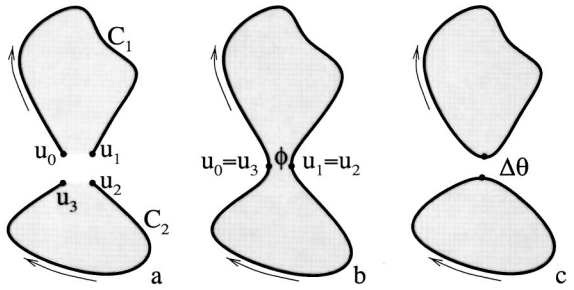

FIG. 2. The auxiliary edge configuration (a) is used to calculate the quadratic part of the action for the tunneling geometries (b), (c). It is assumed that the short-distance cutoff for the long-range potential $V(r)$ is much larger than the scale at which the geometries (b) and (c) differ.

The classical solution is uniquely determined by the given values $u_i(\tau)$ of the fields at the endpoints. The quadratic action (2), (3), evaluated along this classical solution, can be written as

$$\mathcal{S}_q[u]=\mathcal{G}[u_1-u_0,u_3-u_2]+\int d\tau\frac{(u_1-u_0)i\partial_\tau(u_1+u_0)}{4\pi}+\int d\tau\frac{(u_3-u_2)i\partial_\tau(u_3+u_2)}{4\pi}, \tag{11}$$

where $\mathcal{G}[a,b]$ is a quadratic, nonlocal in time, and generally a very complicated functional of its arguments.

The conservation of the total charge

$$Q=\frac{\sqrt{\nu}}{2\pi}(u_3-u_2+u_1-u_0) \tag{12}$$

requires that $\varphi\equiv u_1-u_0=u_2-u_3$, up to a time-independent constant. Setting the total charge to zero, we can write Eq. (11) as

$$\mathcal{S}_q[\varphi,\Delta\theta]=\mathcal{G}[\varphi,-\varphi]-\frac{1}{2\pi}\int d\tau\varphi i\partial_\tau\Delta\theta, \tag{13}$$

where $\Delta\theta\equiv(u_3+u_2-u_1-u_0)/2$. For the tunneling geometry in Fig. 2(b), Eq. (12) implies that the field $u(x,\tau)$ can be chosen continuous everywhere along the combined edge C_1+C_2, $\Delta\theta=0$ and hence the effective quadratic action becomes

$$S_q=\mathcal{G}[\varphi,-\varphi]\equiv\frac{T}{4\pi}\sum_{\omega_n=2\pi nT}|\omega_n|\mathcal{K}(\omega_n)|\varphi_n|^2,$$

where we introduced the coupling $\mathcal{K}(\omega)$ as in Eq. (5).

For the tunneling geometry in Fig. 2(c), the charges in upper and lower areas change with time as a result of the tunneling, and we must keep the field $u(x,\tau)$ discontinuous. The corresponding action becomes

$$\tilde{S}_q=\frac{T}{4\pi}\sum_n|\omega_n|\mathcal{K}(\omega_n)|\varphi_n|^2+\omega_n(\overline{\varphi}_n\Delta\theta_n-\Delta\overline{\theta}_n\varphi_n).$$

(Note that a different choice of $\Delta\theta$, e.g., $\Delta\theta=u_3-u_0$ or $\Delta\theta=u_2-u_1$, only changes the Euclidean Lagrangian by a total time derivative, thus leaving the action $\tilde{S}_q$ invariant.)

The field φ can be now trivially integrated out, and we arrive at the final form of quadratic action for this geometry,

$$\tilde{S}_q=\frac{T}{4\pi}\sum_{\omega_n}|\omega_n|\tilde{\mathcal{K}}(\omega_n)|\Delta\theta_n|^2,\quad \tilde{\mathcal{K}}(\omega_n)=\frac{1}{\mathcal{K}(\omega_n)}. \tag{14}$$

This result can be generalized for systems with several junctions, where the coupling $\mathcal{K}(\omega)$ is replaced by a matrix, which is inverted when all junctions are replaced by their duals.[28]

This simple calculation shows that even in the presence of long-range interactions the duality between weak tunneling and weak backscattering for the model described by Eqs. (2), (3), (4) coincides with the duality between weak and strong coupling for the effective tunneling model (5), independent of the actual geometry of the system. The only assumption we made is that the geometries in Fig. 2(b) and Fig. 2(c) should not differ ''substantially,'' that is, the size of a junction near a saddle point should be sufficiently small (e.g., compared with a short-distance cutoff length, or, at small enough frequencies, with the wavelength v/ω), so that the Coulomb potential would be the same in the points $u_0,\ldots,u_3$.

IV. SCALE-INVARIANT MODELS

In the absence of long-range forces ($e^2=0$), the properties of any system are determined only by the relative location of the tunneling points along the edges. If such a system has only one tunneling point, in the limit where both contours C_1 and C_2 in Fig. 2 become infinite, the system would not ''know'' the difference between the geometries in Figs. 2(b) and 2(c), and the duality implies that the coupling has a universal self-dual value $\mathcal{K}(\omega)=1$, independent of the actual geometry of the edges. Of course, this statement requires that $\omega L/v\gg 1$, otherwise one can obtain[28] for Figs. 2(b) and 2(c), respectively,

$$\mathcal{K}^{(2b)}=[\mathcal{K}^{(2c)}]^{-1}=\frac{1}{2}\left|\coth\left(\frac{\omega L_1}{2v}\right)+\coth\left(\frac{\omega L_2}{2v}\right)\right|,$$

where L_i is the length of the contour C_i, and a uniform edge velocity $v(x)=v$ is assumed for simplicity.

In the presence of Coulomb interactions, the functional form $\mathcal{K}(\omega)$ has been previously found[23–25] only for two *parallel* edges ($\alpha\to 0$ or $\alpha=\pi$ in Fig. 1), where the translational symmetry of the quadratic part of the action is restored. In any other geometry the distance $|x-y|$ measured along the edges, and the geometrical distance $R_{xy}\equiv|\mathbf{r}_x-\mathbf{r}_y|$ in Eq. (3) are no longer equivalent, and an analytic computation of the average (6) with ''noninteracting'' quadratic action $\mathcal{S}_0+\mathcal{S}_1$ becomes virtually impossible.

Some simplification can be achieved for an idealized *X*-shaped geometry (see Fig. 1), which can be also introduced as the zero-bias limit of the edges in a vicinity of a saddle point with the opening angle α. The duality discussed in the previous section implies that $\mathcal{K}_{\pi-\alpha}(\omega)=\mathcal{K}_\alpha^{-1}(\omega)$, for a given edge velocity $v(x)$ and a given form of long-range potential $V(R)$. Therefore, in the self-dual geometry at $\alpha=\pi/2$, we expect $\mathcal{K}_{\pi/2}=1$ exactly, independent of the form or the strength of $V(R)$.

For the special case of unscreened Coulomb potential,

$$V(R)=(R^2+a^2)^{-1/2}, \tag{15}$$

the long-range interaction term (3) scales the same way as the local potential (velocity) term in Eq. (1). Then, if the edge velocity $v(x)=v$ is coordinate independent, simple scaling shows that frequency can only enter in the dimensionless combination $\bar{\omega}=\omega a/v$, while the strength of the Coulomb interaction is defined by the dimensionless coupling constant[23]

$$\chi\equiv\nu e^2/(\pi\hbar v\varepsilon). \tag{16}$$

Therefore, the tunneling properties of the junction [i.e., the form of the dimensionless function $\mathcal{K}_\alpha(\omega)$] are fully determined by three dimensionless parameters, namely,

$$\mathcal{K}_\alpha(\omega;a,v,e^2)=K_\alpha(\bar{\omega};\chi).$$

On general grounds one can argue that in the scale-invariant limit $\bar{\omega}\ll 1$ the function $K_\alpha(\bar{\omega};\chi)$ can depend on its first argument at most logarithmically.

To rewrite more explicitly the general Coulomb action (3) for the infinite geometry in Fig. 1, let us introduce the coordinate x along each edge, with the origin at the tunneling point and positive direction to the right. Then the charge densities along the top and the bottom boundaries are respectively $\rho_1(x)=\sqrt{\nu}\partial_x u_1(x)/(2\pi)$ and $\rho_2(x)=-\sqrt{\nu}\partial_x u_2(x)/(2\pi)$ (the sign in the second expression differs because the coordinate is now chosen in the direction opposite to the edge velocity). The Coulomb part of the action becomes

$$\mathcal{S}_1=\frac{\chi}{8\pi}\int d\tau\int_{-\infty}^{\infty}dx\,dy\sum_{i,j=1,2}(-1)^{i+j}\partial_x u_i V_{ij}(x,y)\partial_y u_j,$$

where the potential $V_{ij}(x,y)\equiv V(|\mathbf{r}_i(x)-\mathbf{r}_j(y)|)$ denotes the interaction energy between unit charges at the points x and y at the edges i and j, respectively, and we changed the units of distance: from now on $v=1$. For symmetric geometries $V_{ij}(x,y)=V_{ij}(y,x)$, $V_{11}(x,y)=V_{22}(x,y)$, and the obtained expression can be diagonalized by introducing the symmetric and antisymmetric combinations $\varphi=u_1-u_2$, $\vartheta=u_1+u_2$. The quadratic part (2), (3) of the Euclidean action becomes

$$\mathcal{S}_q=\frac{T}{8\pi}\sum_n\left\{\int dx[2\omega_n\bar{\varphi}(x)\vartheta_x'+|\varphi_x'|^2+|\vartheta_x'|^2]+\frac{\chi}{2}\int dx\int dy[\bar{\varphi}_x'V_+(x,y)\varphi_y'+\bar{\vartheta}_x'V_-(x,y)\vartheta_y']\right\}, \tag{17}$$

where $V_\pm(x,y)\equiv V_{11}(x,y)\pm V_{12}(x,y)$ and the coordinate integrations are performed along the entire real axis. Note that the first term of the integrand is not written as $\omega_n(\bar{\varphi}\vartheta_x'-\bar{\vartheta}\varphi_x')$ as would be expected from the action (1); the integrand in Eq. (17) differs by a full spatial derivative, exactly equivalent to the surface term in the second line of Eq. (2).

The interaction potential is always an even function with respect to simultaneous reflection of both coordinates, $V_\pm(x,y)=V_\pm(-x,-y)$, and the fields $\varphi=\varphi_s+\varphi_a$ and ϑ

$=\vartheta_s+\vartheta_a$ can be separated into symmetric (s) and antisymmetric (a) components. The first term of the action (17) couples only the components of two fields with the opposite symmetry: φ_s with ϑ_a, and φ_a with ϑ_s. Since the tunneling term depends on the field $\varphi(0)=\varphi_s(x=0)$ only, the components $\varphi_a(x)$ and $\vartheta_s(x)$ decouple and can be integrated out independently of the value $\varphi(0)$. In the following, we shall presume that this symmetrization has been done, and use

$$\varphi(x)=\varphi(-x), \quad \vartheta(x)=-\vartheta(-x), \tag{18}$$

with the indices ''s'' and ''a'' dropped for convenience.

A. Exactly solvable example

To illustrate the properties of the symmetrized action (17), consider a model problem where the interaction happens only between the points at equal distance from the origin,

$$(\chi/2)V_{11}(x,y)=v_0\delta(x-y)+v_1\delta(x+y),$$

$$(\chi/2)V_{12}(x,y)=v_2\delta(x-y)+v_3\delta(x+y),$$

where the velocity v_0 (measured in units of bare velocity v) denotes the strength of additional interaction at the same edge, v_1 and v_2 denote the interaction between the neighboring edges (left–right and top–bottom), while v_3 denotes the interaction between the points at the opposing edges. (Physically, this set of interactions corresponds to four locally interacting chiral edges, running along the surface of a semi-infinite cylinder and meeting in the tunneling point at its near end).

With interaction of this simple form we can use the symmetry properties (18), and the quadratic action (17) becomes entirely *local*,

$$\mathcal{S}_q=\frac{T}{8\pi}\sum_n \int dx[2\omega_n\overline{\varphi}(x)\partial_x\vartheta+v_\varphi|\partial_x\varphi|^2+v_\vartheta|\partial_x\vartheta|^2],$$

with $v_{\varphi,\vartheta}=1+v_0-v_3\pm(v_1-v_2)$. Now the field $\vartheta(x)$ can be trivially integrated out, and Eq. (6) gives

$$\mathcal{K}^{-1}(\omega_n)=\frac{1+v_0-v_3+(v_1-v_2)}{1+v_0-v_3-(v_1-v_2)}.$$

Clearly, under interchange $v_1\leftrightarrow v_2$ this expression goes to its inverse according to the duality relation derived in Sec. III, and $\mathcal{K}(\omega_n)=1$ for the self-dual case $v_1=v_2$ where all edges are equivalent.

B. Coulomb interactions near a saddle point

Now let us consider more realistic long-distance interactions in the edge geometry shown in Fig. 1. We write the intra- and interedge interaction potentials

$$V_{11}(x,y)=\theta(xy)V(x-y)+\theta(-xy)V(R_\alpha),$$

$$V_{12}(x,y)=\theta(xy)V(R_\alpha)+\theta(-xy)V(x-y),$$

where the bulk distance $R_\alpha\equiv(x^2+y^2-2xy\cos\alpha)^{1/2}$, $\theta(x)$ is the usual step function, $\theta(x)=1$ for $x>0$ and $\theta(x)=0$ otherwise, and $V(x)$ is, e.g., the Coulomb potential (15). The resulting effective action has the form (17), with

$$V_+=V(x-y)+V(R_\alpha), \tag{19}$$

$$V_-=[V(x-y)-V(R_\alpha)]\mathrm{sgn}(xy). \tag{20}$$

In the limit $\alpha=0$, $R_\alpha=|x-y|$, the antisymmetric part of the potential vanishes, $V_-(x,y)=0$, while $V_+(x,y)=2V(x-y)$, and we obtain the usual translationally invariant action for two parallel edges. Integrating out the field ϑ and diagonalizing the remaining part of the action with the help of Fourier transformation, we use Eq. (6) to calculate the coupling,

$$\mathcal{K}^{-1}_{\alpha=0}(\omega)=\frac{2\overline{\omega}}{\pi}\int_0^\infty\frac{d\zeta}{\overline{\omega}^2+\zeta^2[1+2\chi K_0(\zeta)]}, \tag{21}$$

where the Fourier-transformed Coulomb potential (15), $V(\zeta)=2K_0(\zeta)$, is expressed in terms of the modified Bessel function K_0, and the reduced frequency $\overline{\omega}=a\omega/v$. Performing the integration with logarithmic accuracy, we obtain, in agreement with Refs. 23–25

$$\mathcal{K}_{\alpha=0}=\left[1+2\chi\ln\left(\frac{2\sqrt{2\chi}e^{-\gamma}}{\overline{\omega}}\right)\right]^{1/2}+\mathcal{O}(|\ln\overline{\omega}|^{-1/2}), \tag{22}$$

where $\gamma\approx0.577$ is the Euler constant.

The case $\alpha=\pi$ corresponds to two semi-infinite nonchiral Luttinger liquids connected by a tunneling point ($\alpha\to\pi$ in Fig. 1); by duality we expect[25] $\mathcal{K}_{\alpha=\pi}=1/\mathcal{K}_{\alpha=0}$. This expression is proved again, specifically for this geometry, in Appendix A.

We argued that in the self-dual case $\alpha=\pi/2$, $\mathcal{K}(\omega)=1$ identically, independently of the properties of the potential $V(R)$, as long as it is appropriately regularized at short distances. We have also constructed a direct analytical solution for this case. The major simplification comes from an observation that the potential $V(R_{\pi/2})=V(\sqrt{x^2+y^2})$ is a symmetric function of x and y independently; the corresponding contribution vanishes from the action (17) by the symmetry (18). As a result, only the potentials $V(x\pm y)$ with the distance measured along the edge enter the extremum equations, and these equations can be solved exactly using the Wiener-Hopf method, as detailed in Appendix B. This direct solution confirms the universal result $\mathcal{K}_{\alpha=\pi/2}=1$. In addition, the explicitly found extremum configuration of the fields $\varphi(x)$, $\vartheta(x)$ is used to get a perturbative expression for $\mathcal{K}_\alpha(\omega)$ near the self-dual point $\alpha_0=\pi/2$. This yields (see Appendix B)

$$\mathcal{K}_\alpha(\omega\to0)\approx1+\mathcal{N}(\chi)\chi\cos\alpha, \quad |\cos\alpha|\ll1, \tag{23}$$

where $\mathcal{N}(\chi)$ is *independent of* ω. In the limit of weak Coulomb interactions, $\mathcal{N}(\chi\to0)\approx1.51$, while $\mathcal{N}(\chi=1.0)\approx0.21$.

To get a handle on the dependence of the coupling $\mathcal{K}_\alpha(\omega)$ on the parameters and the cutoff scales, we have also evaluated the average (6) numerically for the quadratic action (17) with the Coulomb potential (15) at different frequencies ω, and for different values of the angle α and the dimensionless coupling constant χ.

To perform this calculation we wrote a discretized version of the quadratic action (17) in terms of lattice values $\varphi(x_n)$ and $\vartheta'(x_n)$, $0<n<N-1$, and then integrated out the values of the fields away from the origin, which only required in-

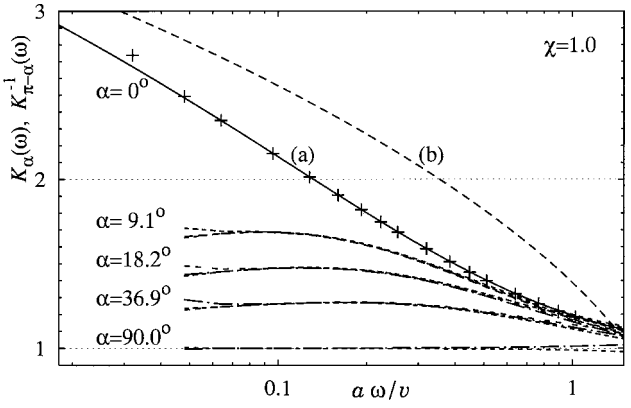

FIG. 3. Superimposed values of $K_\alpha(\bar{\omega})$, $K^{-1}_{\pi-\alpha}(\bar{\omega})$ calculated numerically for the Coulomb potential (15) at different values of the opening angle α, with $L=20$ and the lattice size $N=1600$. The self-duality of the original action (17) is violated by the finite system size L at small $\bar{\omega}\equiv a\omega/v$, and by the discreteness of the lattice spacing at large $a\omega/v$. Pluses show the numerical data at $\alpha=0$, while the lines (a) and (b) respectively, correspond to Eqs. (21) and (22) in the text.

verting two $N\times N$ matrices. In addition to the cutoff distance a in Eq. (15), the discretization involved two explicit cutoff scales: the total system size L and the lattice grid size $h=L/N$. The calculations were performed in the regime $h\ll a\ll L$; the results are independent of these cutoff scales in the frequency range $h\ll v/\omega\ll L$. These inequalities substantially limited the dynamical range where the results are accurate.

Typical results of the calculations are illustrated in Figs. 3 and 4. The curves in Fig. 3 with marked values of α show superimposed values $K_\alpha(\bar{\omega})$, $K^{-1}_{\pi-\alpha}(\bar{\omega})$ calculated with the lattice size $N=1600$, for cutoff parameters $a=0.05$, 0.1. A slight deviation between the superimposed curves shows that our discretization violated the self-duality of the problem at both large and small cutoff scales. Nevertheless, as illustrated in Fig. 4, the self-duality holds with a very good numerical accuracy near the middle of the dynamical range, $a\omega/v\sim 0.1$.

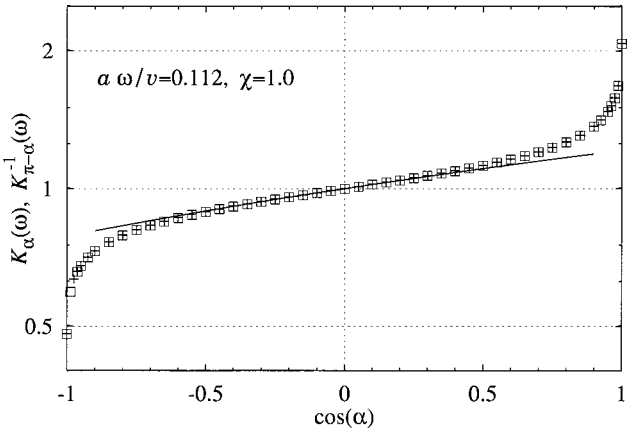

FIG. 4. Duality for junctions in Fig. 1 illustrated numerically. Boxes and pluses show the superimposed values $K_\alpha(\bar{\omega})$ and $K^{-1}_{\pi-\alpha}(\bar{\omega})$, calculated with the Coulomb potential (15) at the lattice size $N=1600$, $L=20$. Solid line with the slope $\mathcal{N}(\chi=1)\approx 0.212$ is a fit to the data.

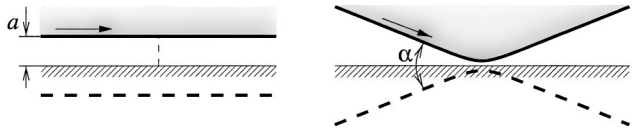

FIG. 5. Two idealized geometries for calculating the effect of Coulomb interactions in cleaved-edge experiments. Edge quasiparticles interact with image charges induced on the metallic surface.

As indicated by finite-size scaling analysis of our data (not shown), at small enough $\bar{\omega}$, $K_\alpha(\bar{\omega})$ saturates to a frequency-independent value in the range $0<\alpha<\pi$. This behavior is consistent with the small-angle expansion (23). In addition, Fig. 4 indicates that Eq. (23) provides a good approximation to $\mathcal{K}_\alpha(\omega)$ in a rather wide range of α. For small $\alpha\ll 1$, as the frequency is reduced, the numerical values $K_\alpha(\bar{\omega})$ seem to closely follow the logarithmically divergent line (21), but eventually cross over to a constant value $K_\alpha(\bar{\omega}=0;\chi)$, which (logarithmically) depends on the angle.

C. Coulomb interactions in the cleaved-edge geometry

Here we consider the effect of long-range interactions in the cleaved-edge geometry,[19,20] where the tunneling happens between a three-dimensional (3D) metal and the edge of a 2DEG, located in the plane perpendicular to the surface of the metal. It is believed that the tunneling in these experiments is dominated by localized ''hot'' spots or impurities. Chamon and Fradkin[34] demonstrated that in the absence of interactions, a point contact between a 3D metal and a QH edge with the filling fraction ν is equivalent to a point tunneling junction between such an edge and an ideal noninteracting $\nu=1$ edge; furthermore, they mapped this latter problem to that of tunneling between two identical edges with filling fractions $\nu_*=2\nu/(1+\nu)$.

The effect of the Coulomb interaction in this setup is limited to the chiral Luttinger liquid, the ''real'' quantum Hall edge, while the Fermi-liquid nature of quasiparticles in the metal imply that they remain noninteracting for the purposes of tunneling measurements. The metallic surface only provides additional screening charges, which modify the form of the interaction potential $V(|\mathbf{r}_x-\mathbf{r}_y|)$. Assuming characteristic frequencies at the edge are small compared with the plasma frequency of electrons in metal (which is always true for a good metal), the retardation can be neglected, and the modified interaction potential is obtained simply by adding the appropriate image charges.

The quadratic part of the action for the translationally invariant geometry shown in the left part of Fig. 5 (i.e., the case $\alpha=0$) is obtained by combining Eq. (2) with the Coulomb energy

$$\mathcal{S}_1=\frac{\chi}{8\pi}\int_0^\beta d\tau\int_{-\infty}^{\infty}dx\,dy\;\partial_x u\hat{V}(x-y)\partial_y u, \qquad (24)$$

where $\hat{V}(x)\equiv V(x)-V(\sqrt{x^2+4a^2})$ is corrected for the image potential, and the units of length are again chosen so that the edge velocity $v=1$. Because we work with the chiral field now, the surface term in the second line of Eq. (2) is absolutely essential even in an infinite geometry. To properly account for this term, we formally separate the field $u=\phi$

$+\theta$ into its symmetric $\phi(x,\tau)=\phi(-x,\tau)$ and antisymmetric $\theta(x,\tau)=-\theta(-x,\tau)$ compontents; then the surface term can be absorbed after an integration by parts, and the action (2) becomes

$$\mathcal{S}_0=\frac{1}{4\pi}\int d\tau\int_{-\infty}^{\infty}dx[2i\partial_\tau\phi\,\partial_x\theta+(\partial_x\phi)^2+(\partial_x\theta)^2]. \tag{25}$$

This transformation is equivalent to ''folding'' the chiral edge in half, which produces two nonchiral fields defined on a semiaxis, and simultaneously eliminates the zero mode and associated subtleties. The translationally invariant action can be now diagonalized by a Fourier transformation, and, after integrating out the fluctuations away from the origin, we obtain the single-edge contribution to the quadratic part of the effective action,

$$\mathcal{S}_q^{(1)}=\frac{T}{2\pi}\sum_n|\omega_n|\hat{\mathcal{K}}(\omega_n)|\phi_1|^2, \tag{26}$$

where $\phi_1\equiv u(0)=\phi(0)$ by definition, and

$$\hat{\mathcal{K}}^{-1}(\omega)=\frac{2|\omega|}{\pi}\int_0^\infty\frac{dk\,Z(k)}{\omega^2+k^2Z^2(k)}, \tag{27}$$

$$Z(k)=1+\frac{\chi}{2}\hat{V}(k).$$

The argument[34] that a point contact with a metal is equivalent to that with a noninteracting $\nu=1$ edge holds independently of the interactions affecting the ''real'' edge. Therefore, the full effective action can be written as

$$\mathcal{S}=\frac{T}{2\pi}\sum_n|\omega_n|(\hat{\mathcal{K}}|\phi_1|^2+|\phi_2|^2)+\int d\tau\,\mathrm{Re}\,\lambda e^{i(g\phi_1-\phi_2)}, \tag{28}$$

where we used $\hat{\mathcal{K}}=1$ for the auxiliary $\nu=1$ edge. The canonical form (5) of the tunneling action can be obtained by introducing the tunneling degree of freedom $\varphi=g\phi_1-\phi_2$ with the corresponding effective coupling $\mathcal{K}_{\rm eff}$ calculated, e.g., using the average as in Eq. (6). As before, the resulting model describes an overdamped particle in a washboard potential; the corresponding non-Ohmic ''friction'' coefficient

$$\kappa_{\rm eff}(\omega)\equiv\frac{\mathcal{K}_{\rm eff}}{g_{\rm eff}^2}=\frac{2}{g^2/\hat{\mathcal{K}}(\omega)+1}. \tag{29}$$

In the noninteracting limit $\hat{\mathcal{K}}(\omega)=1$ this expression safely goes into the result[34] obtained by a different method.

Notice that the long-distance part of the Coulomb potential $\hat{V}$ in Eq. (24) is screened by the metallic surface. Then, at sufficiently small frequencies, $a\omega\ll v_{\rm r}\equiv Z(0)v$, the momentum dependence of the coefficient $Z(k)$ can be ignored, and the integral (27) gives precisely the noninteracting coupling, $\hat{\mathcal{K}}=1$. This is not at all surprising, since the interaction happens within a single chiral edge, and its long-range part (most dangerous at small frequencies) is screened. As usual,[35] the only effect of the additional interaction in this chiral system is the velocity renormalization, $v\to v_{\rm r}$.

The translational symmetry is lost for the ''wedge'' geometry shown in the right part of Fig. 5. The Coulomb part of the corresponding action can be written in the form (24) with the potential $\hat{V}(x-y)\to V_-(x,y)$ given by Eq. (20). In the limit $\alpha\to 0$, the potential $V_-(x,y)$ vanishes identically, and hence $\hat{\mathcal{K}}(\omega)=1$ in this case as well.

At general values of α we again use the ''folding'' trick by introducing symmetric and antisymmetric variables ϕ, θ. Up to an overall coefficient, the resulting action looks like Eq. (17), with the exception that both components ϕ and θ couple with the *same* potential $V_-(x,y)$. The most prominent difference is that at $\alpha=\pi/2$ the symmetry no longer leads to a cancellation of the part $V(\sqrt{x^2+y^2})$ of the total potential, and the effect of the long-distance interactions is no longer trivial, $\hat{\mathcal{K}}_{\pi/2}(\omega)\neq 1$. Again, this comes as no surprise, since there is no self-duality in this geometry.

Finally, in the limiting case $\alpha=\pi$, the potential $V_-(x,y)$ becomes an even function of each argument; as a result, the coupling with the symmetric field ϕ (antisymmetric derivative $\partial_x\phi$) vanishes by symmetry. Up to an overall coefficient, the resulting action is identical to that considered in Appendix A, and we obtain [note that the extra coefficient was already accounted for in the corresponding effective action, cf. Eqs. (26) and (5)],

$$\hat{\mathcal{K}}_{\alpha=\pi}(\omega)=\mathcal{K}_{\alpha=\pi}(\omega)=\frac{2|\omega|}{\pi}\int_0^\infty\frac{dk}{\omega^2+k^2(1+\chi V(k))}.$$

This result is quite intuitive: metallic screening becomes noneffective in the case where a wire is perpendicular to the conducting surface.

Our calculations imply that the tunneling exponent is modified by the Coulomb interaction only if the edge is bent near the tunneling point. In an ideal sample, the edge runs along a straight line parallel to the surface of the metal, and long-range interactions do not modify the tunneling exponents. In any real sample, however, imperfections near the tunneling point always reduce the effective coupling $\mathcal{K}(\omega)$, or, equivalently, systematically *increase* the tunneling exponent in Eq. (10). Nevertheless, we do not believe this effect would be sufficient to explain a 10% increase of the tunneling exponent observed[20] by Grayson *et al.* near $\nu=1$: cleaved-edge samples are characterized by sharp confinement and large drift velocities, meaning that the corresponding dimensionless coupling constant χ [see Eq. (16)] is small.

V. DISCUSSION

We have shown that the effect of long-range interactions on transport through a QH tunneling junction depends crucially on its geometry. In particular, in a self-similar *X*-shaped junction (see Fig. 1) characterized by an opening angle α, unscreened Coulomb interactions renormalize the effective Luttinger-liquid exponent,

$$g_\star^2=g^2/\mathcal{K}_\alpha(\omega=0;\chi),$$

where $g^2=1/\nu$ for electron tunneling between the edges of 2DEGs with Laughlin fractions ν. Therefore, the renormal-

ized exponent depends nonuniversally on the angle α and the dimensionless Coulomb interaction strength χ.

This implies that the system should exhibit a zero-temperature delocalization transition at a critical angle characterized by $g_\star^2=1$. This is in contrast with the transport properties expected in the absence of long-range interactions, which are exclusively determined by the filling fraction ν. For integer QH systems with $\nu=1$, the transition always corresponds to a self-dual geometry, i.e., $\alpha_c=\pi/2$, independently of the details of the interaction. In fractional QH constrictions, however, the transition (if any) occurs at a nonuniversal critical angle $\alpha_c<\pi/2$, such that $\mathcal{K}_{\alpha_c}(0;\chi)=\nu^{-1}$.

Properties of all charge transfer processes through the junction are defined by the parameter $g_\star$ in the effective action (13), which determines the tunneling exponents[5,7] [see Eq. (10)], the form of the nonlinear *I-V* curve,[8,9] as well as the tunneling noise.[10–12] In the limit of weak tunneling, the quantization of transferred charge is ultimately determined by gauge invariance, and a shot-noise measurement would show current transferred by unit charges. However, the shot noise measured in the opposite, strongly coupled limit (reached, e.g., by driving a large tunneling current through the junction) is set[36] by the instanton charge for the effective tunneling action (13). The value of this charge is determined solely by the value of $g_\star$. Hence, in this regime a noise measurement would show a nonuniversal charge

$$e_\star/e=1/g_\star^2=\nu\mathcal{K}_\alpha(0;\chi),$$

clearly an interaction effect.

The described situation applies to ideal systems without screening. More realistically, Coulomb interactions are screened at some finite length ξ. Then, for a junction with finite opening angle, $|\cos\alpha|<1$, the correction to tunneling exponents always vanishes in the static limit, $\mathcal{K}_\alpha^{(\mathrm{scr})}(0)=1$, even though it may be significant at larger frequencies, $\omega\gtrsim v/\xi$ (this corresponds to a temperature 0.1 K for $\xi=1\,\mu$m and $v=10^7$ cm/s). Consequently, a system at a fractional ν with originally metallic behavior would eventually localize at small enough temperatures.[23,25] Contrarily, the interaction-induced flow in an integer junction would gradually stop without changing its direction.

For an *X*-shaped junction with a given opening angle α, the magnitude of the renormalization parameter $\mathcal{K}_\alpha(0;\chi)$ is determined by the value of the dimensionless Coulomb interaction constant (16), which, in turn, is defined by the edge wave (drift) velocity. For mesaetched samples with expectedly sharp confining potential, edge magnetoplasmon velocities have been measured[37] by Ashoori *et al.*, yielding $v\sim10^8$ cm/s, which corresponds to $\chi\sim0.05$. On the other hand, edge electric fields equivalent to drift velocities as small as $v\sim10^6$ cm/s have been measured by Maasilta and Goldman,[14] who analyzed discrete energy levels of a quantum antidot. This value of velocity results in a relatively large coupling constant value $\chi\sim5$.

We must point out, however, that our discussion of Coulomb interaction effects was based on a single-mode sharp edge, which implies large confining electric fields of order $\mathcal{E}\sim E_g/(el)$, where E_g is the energy gap associated with the incompressible QH state, and l is the magnetic length. Using the drift velocity $v=c\mathcal{E}/B$, we obtain

$$\chi=\frac{\nu e^2}{\pi\varepsilon\hbar v}\sim\left(\frac{\nu e^2}{\pi\varepsilon l}\right)E_g^{-1}, \tag{30}$$

which, for a typical QH sample, leads to $\chi\lesssim1$. Samples with much larger values of the Coulomb coupling (small v, soft confinement) are likely to have a tendency to edge reconstruction.[18] This would lead to additional polarization at the edge due to neutral modes, and, consequently, a partial screening of Coulomb interaction.

Therefore, to observe the predicted effects, samples with well-defined, but not too sharp edges are necessary. This excludes the cleaved-edge samples (where the drift velocity v is large), as well as the samples with electrostatically defined geometry (where confinement tends to be soft). The best choice would therefore be a Hall bar with lithographically defined *X*-shaped constriction and a narrow local gate to fine tune the tunneling. For a given base temperature T, the linear size of the constriction should be at least of order $\xi\sim\hbar v/T$, i.e., approaching a millimeter scale for a mK temperature range. Tunneling junctions with small opening angles will give larger values of $\mathcal{K}_\alpha$ [in principle, limited only by the logarithm (22), divergent at small frequencies]. However, as illustrated in Fig. 3, for such junctions the renormalized Luttinger parameter $g_\star^2$ is more likely to retain some frequency (temperature) dependence, which would modify the measured exponents.

ACKNOWLEDGMENTS

We gratefully acknowledge useful discussions with C. de C. Chamon, M. Fogler, C. Glattli, E. Gwinn, S. A. Kivelson, D.-H. Lee, Z. Nussinov, S. L. Sondhi, and X.-G. Wen. A.A. acknowledges support of the Israeli Science Foundation and the fund for Promotion of Research in the Technion. E.S. acknowledges support by Grant No. 96–00294 from the United States–Israel Binational Science Foundation (BSF), Jerusalem, Israel. L.P.P. was supported in part by DOE Grant No. DE-FG02-90ER40542.

APPENDIX A: COUPLING AT $\alpha=\pi$

Here we derive the form of the coupling $\mathcal{K}(\omega)$ for the saddle-point geometry shown in Fig. 1 in the special limit $\alpha=\pi$, which corresponds to two vertical semi-infinite wires connected by a single tunneling point. In this case the distance $R_\alpha=|x+y|$, and the contribution of the symmetric potential $V_+(x,y)=V(x-y)+V(x+y)$ to Eq. (17) vanishes by symmetry (18), so that only the part $V_-(x,y)=[V(x-y)-V(x+y)]\mathrm{sgn}(xy)$ remains. The symmetry of the derivative $\partial_x\vartheta$ implies that both parts of the potential V_- give identical contribution, and the quadratic part of the action (17) can be written as

$$\mathcal{S}_q=\frac{T}{8\pi}\sum_n\left\{\int_{-\infty}^{\infty}dx[2\omega_n\overline{\varphi}(x)\partial_x\vartheta+|\partial_x\varphi|^2+|\partial_x\vartheta|^2]\right.$$
$$\left.+\chi\int_{-\infty}^{\infty}dx\,dy[\partial_x\overline{\vartheta}V(x-y)\partial_y\vartheta\,\mathrm{sgn}(xy)]\right\}. \tag{A1}$$

Unlike the case $\alpha=0$, the nonlocal interaction in the second line cannot be diagonalized by a simple Fourrier transformation; we need to get rid of the sign function first. Naively,

this could be done by multiplying both $\varphi(x)$ and $\vartheta(x)$ by $\mathrm{sgn}(x)$. However, since $\varphi(0)\neq 0$, the function $\varphi(x)\mathrm{sgn}(x)$ would not be continuous at the origin, so that spurious δ functions may be generated. Instead, we define auxiliary continuous functions $u(x)$, $g(x)$, so that

$$\varphi(x)=\varphi(0)+\mathrm{sgn}(x)u(x), \quad g(x)=\vartheta(\infty)-\mathrm{sgn}(x)\,\vartheta(x),$$

and $u(0)=g(\infty)=0$. After integrating out the field $u(x)$, the effective action becomes

$$\mathcal{S}_q=\frac{T}{8\pi}\sum_n \left\{-4\omega_n\overline{\varphi}(0)g(0)+\int\frac{dk}{2\pi}|g_k|^2[\omega_n^2+k^2 \times(1+\chi V(k))]\right\}.$$

In the first term here we substitute $g(0)=\int dk\, g_k/(2\pi)$ in terms of the Fourier-transformed field g_k, integrate this field out, and obtain the effective action for the the field $\varphi(0)$ alone,

$$\mathcal{S}_q=\frac{T}{4\pi}\sum_n \omega_n|\varphi(0)|^2\left[\frac{2\omega_n}{\pi}\int_0^\infty\frac{dk}{\omega_n^2+k^2(1+\chi V(k))}\right];$$

comparing the result with the general form of the effective action (5), and the result (21) for $\alpha=0$, we conclude that

$$\mathcal{K}_{\alpha=0}(\omega_n)\mathcal{K}_{\alpha=\pi}(\omega_n)=1$$

exactly, independent of the form of the potential $V(x)$.

APPENDIX B: SELF-DUAL TUNNELING JUNCTION, $\alpha=\pi/2$

1. General Wiener-Hopf solution

Here we give a direct solution of the extremum equations for the self-dual case $\alpha=\pi/2$. This solution gives the coupling $\mathcal{K}_{\pi/2}=1$ directly, without utilizing the self-duality of the problem. In addition, it allows us to calculate $\mathcal{K}_\alpha$ perturbatively for small values of $|\cos(\alpha)|\ll 1$.

Begin with the Euclidean action (17) at $\alpha=\pi/2$,

$$\mathcal{S}_q=\frac{T}{8\pi}\sum_n\int dx\left\{2\omega_n\overline{\varphi}(x)\,\vartheta_x'+\int dy\,\overline{\varphi_x'}Z(x-y)\varphi_y' + \int dy\,\overline{\vartheta_x'}Z(x-y)\mathrm{sgn}(xy)\,\vartheta_y'\right\}, \tag{B1}$$

where the total potential

$$Z(x-y)=\delta(x-y)+\frac{\chi}{2}V(x-y); \tag{B2}$$

note that due to the symmetry (18), the contribution from the part of the potential with geometrical distance $V(R_{\pi/2})=V(\sqrt{x^2+y^2})$ was cancelled. The Euler-Lagrange equations (valid at $x\neq 0$, where the nonlinear tunneling term gives no contribution) are

$$\omega\partial_x\vartheta-\partial_x\int_{-\infty}^{\infty}dy\,Z(x-y)\partial_y\varphi=0, \tag{B3}$$

$$\omega\partial_x\varphi-\partial_x\int_{-\infty}^{\infty}dy\,Z(x-y)\mathrm{sgn}(xy)\partial_y\vartheta=0. \tag{B4}$$

We assume that both fields are continuous everywhere, and that $\varphi(x)$ and $\partial_x\vartheta(x)$ vanish at infinity. Multiplying the first of the obtained equations by $\overline{\varphi}(x)$, the second by $\overline{\vartheta}(x)$, and subtracting the results from the integrand in the action (B1), with the help of the definition (B2) we obtain

$$\mathcal{S}_q=\frac{T}{8\pi}\sum_n\int dx\,\partial_x\Big[\omega_n\overline{\varphi}\vartheta+\overline{\varphi}(x)\int dy\,Z(x-y)\partial_y\varphi + \overline{\vartheta}(x)\int dy\,Z(x-y)\mathrm{sgn}(xy)\partial_y\vartheta\Big] = -\frac{T}{8\pi}\sum_n\overline{\varphi}(0)\Delta\varphi_0',$$

$$\Delta\varphi_0'\equiv\varphi'(0_+)-\varphi'(0_-), \tag{B5}$$

where the integration was performed over the entire axis excluding the point $x=0$. The Euler-Lagrange equations (B3), (B4) can be simplified by defining linear combinations (symmetric with respect to x)

$$A,B(x)=[\varphi(x)\pm\vartheta(x)\mathrm{sgn}(x)]/2, \tag{B6}$$

then, multiplying Eq. (B4) by $\mathrm{sgn}(x)$ and taking symmetric and antisymmetric combinations of the result with Eq. (B3), we obtain at $x\neq 0$

$$\omega\,\mathrm{sgn}(x)\partial_x A-\partial_x\int_{-\infty}^{\infty}dy\,Z(x-y)\partial_y A=0, \tag{B7}$$

and an identical equation (up to the substitution $\omega\to-\omega$) for $B(x)$. We integrate, keeping in mind that Eq. (B7) is valid for $x\neq 0$,

$$\omega A\,\mathrm{sgn}(x)-\int_{-\infty}^{\infty}dy\,Z(x-y)\partial_y A=C_a\mathrm{sgn}(x), \tag{B8}$$

where the integration constants in the intervals $x<0$ and $x>0$ were related using the symmetry $A(x)=A(-x)$. The value of the constant C_a is determined by the boundary conditions; using the definition (B6) we obtain

$$2C_a=\omega\varphi(0)-\varphi'(0_+)-\vartheta'(0)=\omega\vartheta(\infty). \tag{B9}$$

Similarly, the integration of the corresponding equation for the function $B(x)$ yields

$$2C_b=-\omega\varphi(0)-\varphi'(0_+)+\vartheta'(0)=\omega\vartheta(\infty). \tag{B10}$$

Together, Eqs. (B9) and (B10) imply that

$$C_a=C_b=-\varphi'(0_+)/2. \tag{B11}$$

Because of the sign function multiplying the first term on the left hand side (LHS), Eq. (B8) cannot be solved directly by a Fourier transformation. It is, however, of the form solvable by the Wiener-Hoph technique.[38] Following the standard prescription, we introduce the functions $A_\pm(x)$

$=A(x)\theta(\pm x)$, so that, e.g., $A(x)=A_+(x)+A_-(x)$, $A(x)\mathrm{sgn}(x)=A_+(x)-A_-(x)$. After this substitution we can Fourier transform Eq. (B8),

$$\omega[A_+-A_-]+ikZ(k)[A_++A_-]=2iC_a\mathcal{P}\frac{1}{k}, \quad \text{(B12)}$$

where $\mathcal{P}$ denotes the principal value, and the Fourier-transformed functions $A_\pm\equiv A_\pm(k)$ have no singularities above and below the real axis, respectively (regularization at infinity ensures that they are also analytic everywhere along the real axis). The functions $A_\pm(x)$ are only discontinuous in the origin, and the asymptotic form of their Fourier transformations at $|k|\to\infty$ is

$$A_\pm(k)=\pm\frac{i}{k}A_\pm(0_\pm)+\mathcal{O}(|k|^{-2})=\pm i\frac{\varphi(0)}{2k}+\cdots. \quad \text{(B13)}$$

The independent functions in Eq. (B12) can be rearranged as follows,

$$A_+(k)=-\mathcal{R}(k)A_-(k)+\frac{2C_a}{kZ-i\omega}\mathcal{P}\frac{1}{k}, \quad \text{(B14)}$$

$$\mathcal{R}(k)\equiv\frac{kZ+i\omega}{kZ-i\omega}=\frac{\mathcal{R}_-(k)}{\mathcal{R}_+(k)}, \quad \text{(B15)}$$

where the function $\mathcal{R}(k)$ was separated into the ratio of the function $\mathcal{R}_-(k)$, which has neither singularities nor zeros at and below the real axis, and $\mathcal{R}_+(k)$, which has the same properties at and above the real axis. This separation is possible because the function $\mathcal{R}(k)$ is analytic in a vicinity of the real axis [which is correct for any ω, assuming that the interaction potential $V(x)$ is properly regularized at infinity]. In the absence of the long-distance interactions $\chi=0$, the decomposition is trivial $\mathcal{R}^0_\pm=(k\pm i\omega)^{-1}$, where we assume $\omega>0$. At very large values of k the long-distance part of the potential should not matter. Therefore, to ensure the regularity of the decomposition (B15) at $\chi>0$, we can use the Cauchy formula

$$\ln r_\pm(q)=\int_{-\infty}^{\infty}\frac{dk}{2\pi i}\frac{\ln r(k)}{q-k\pm i0}, \quad r_\pm(q)\equiv\frac{\mathcal{R}_\pm(q)}{\mathcal{R}^0_\pm(q)} \quad \text{(B16)}$$

for the ratio $r(k)=\mathcal{R}(k)/\mathcal{R}^0(k)$. Since $r(k)\to1$ at large k, this expression implies that $r_\pm(k)\to1$ (and hence that $\mathcal{R}_\pm\sim1/k$) as $|k|\to\infty$.

Multiplying Eq. (B14) by $\mathcal{R}_+$, and separating the free term of the obtained expression into a sum of functions analytic above and below the real axis, respectively, we obtain

$$A_+(k)\mathcal{R}_+-2C_ah_+=-A_-(k)\mathcal{R}_-+2C_ah_-. \quad \text{(B17)}$$

Here the functions $h_\pm\equiv h_\pm(k)$, analytic in the upper (lower) complex half-plane, are defined so that $h_+(k)+h_-(k)=h(k)$, where

$$h(k)\equiv\frac{\mathcal{R}_+(k)}{kZ-i\omega}\mathcal{P}\frac{1}{k}=\frac{\mathcal{R}_-(k)-\mathcal{R}_+(k)}{2i\omega}\mathcal{P}\frac{1}{k}; \quad \text{(B18)}$$

these functions can be found using the Cauchy formula

$$h_\pm(q)=\mp\frac{1}{2\pi i}\int_{-\infty}^{\infty}dk\frac{h(k)}{q-k\pm i0}. \quad \text{(B19)}$$

We assumed that $\mathcal{R}_\pm(k)$ are nonsingular in the origin (and elsewhere along the real axis), therefore, using the identity $\mathcal{R}_-(0)=\mathcal{R}(0)\mathcal{R}_+(0)=-\mathcal{R}_+(0)$, we obtain

$$h_\pm(k)=\pm i\frac{\mathcal{R}_\pm(k)}{2\omega(k\pm i0)}. \quad \text{(B20)}$$

By construction, the LHS of Eq. (B17) has no singularities at and above the real axis, while its right hand side (RHS) has no singularities at and below the real axis. Therefore, the whole expression is analytic everywhere in the complex plane, and, as long as it is uniformly limited at infinity, it can only be a constant. Moreover, since both sides of Eq. (B17) actually *vanish* at infinity [as follows from Eq. (B13) and the properties of the functions $\mathcal{R}_\pm$, $h_\pm$], this implies that the whole expression can only be zero everywhere at the complex plane k. We obtain

$$A_\pm(k)=2C_a\frac{h_\pm(k)}{\mathcal{R}_\pm(k)}=\pm\frac{iC_a}{\omega(k\pm i0)}, \quad \text{(B21)}$$

and by matching with the asymptotic expansion (B13), we get

$$C_a=\frac{\omega\varphi(0)}{2}, \quad A_\pm(k)=\pm\frac{i\varphi(0)}{2(k\pm i0)}. \quad \text{(B22)}$$

Comparing to Eq. (B11), we obtain

$$\Delta\varphi_0'=2\varphi'(0_+)=-2\omega\varphi(0)$$

and the contribution at the frequency $\omega>0$ to the effective action (B5) becomes

$$\mathcal{S}_q(\omega)=\frac{T}{4\pi}|\omega|\,|\varphi(0)|^2.$$

One can also obtain an identical contribution at $\omega<0$, so that

$$\mathcal{K}_{\alpha=\pi/2}(\omega)=1, \quad \text{(B23)}$$

as expected by the self-duality of the problem.

The analog of Eq. (B7) for the function $B(x)$ differs only by the sign of ω, which leads to a replacement $\mathcal{R}\to1/\mathcal{R}$, $\mathcal{R}_\pm\to1/\mathcal{R}_\pm$. Instead of Eq. (B17) we get

$$B_+(k)\mathcal{R}_+^{-1}-2C_bf_+=-B_-(k)\mathcal{R}_-^{-1}+2C_bf_-. \quad \text{(B24)}$$

By analogy with Eq. (B20), we obtain

$$f_\pm(k)=\mp i\frac{\mathcal{R}_\pm^{-1}(k)}{2\omega(k\pm i0)}. \quad \text{(B25)}$$

By the same analyticity argument, both sides of Eq. (B24) are analytic everywhere in the complex plane; at $|k|\to\infty$ they asymptotically approach a constant value $i\varphi(0)$. Therefore,

$$B_\pm(k)=\pm i\varphi(0)\left[\mathcal{R}_\pm(k)-\frac{1}{2(k\pm i0)}\right],$$

and, combining with Eq. (B22), we can use the definition (B6) to restore the original fields in the extremum,

$$\varphi(x)=\varphi(0)\int\frac{dk}{2\pi i}[\mathcal{R}_-(k)-\mathcal{R}_+(k)]e^{-ikx}, \quad \text{(B26)}$$

$$\vartheta(x)=\mathrm{sgn}(\omega x)[\varphi(0)-\varphi(x)], \quad \text{(B27)}$$

where the $\mathrm{sgn}(\omega)$ in the second line is needed because the case $\omega<0$ is equivalent to the interchange of A and B, which changes the sign of $\theta(x)$.

It is easy to verify that the obtained functions obey the boundary conditions assumed when deriving Eqs. (B5), (B9), (B10). This self-consistency check ensures that the obtained expressions give us the exact formal solution of the problem.

To understand the structure of this solution, let us introduce the expansion

$$\chi V(x)=\sum_{l=1}^{N}\frac{A_l}{a_l}e^{-a_l|x|}, \quad \chi V(k)=\sum_{l=1}^{N}\frac{2A_l}{k^2+a_l^2}, \quad \text{(B28)}$$

which, for sufficiently large N, gives an adequate regularized representation of any non-pathological even function $V(x)$. For example, the Coulomb potential $V(x)=1/|x|$ can be rewritten as follows,

$$\frac{1}{|x|}=\lim_{a\to 0}\frac{a}{1-\exp(-a|x|)}=\lim_{a\to 0}a\sum_{l=0}^{\infty}e^{-al|x|},$$

so that, given a finite a, any partial sum provides a regularization of the form (B28) with $a_l=al$ and $A_l=\chi a^2 l$.

We obtain

$$Z=1+\frac{\chi}{2}V(k)=1+\sum_{l=1}^{N}\frac{A_l}{k^2+a_l^2},$$

$$kZ-i\omega=P_{2N+1}(k)\prod_{l=1}^{N}(k^2+a_l^2)^{-1},$$

where the polynomial

$$P_{2N+1}(k)=\prod_{s=1}^{2N+1}(k-i\kappa_s)$$

has precisely $(2N+1)$ purely imaginary distinct roots $k_s\equiv i\kappa_s\neq 0$. One can also show that for $\omega>0$ exactly N roots lie below the imaginary axis; we shall assume $\kappa_s<0$ for $1<s<N$. The Cauchy integral (B16) is readily evaluated, and we obtain

$$\mathcal{R}_+=\frac{(k-i\kappa_1)\times\ldots\times(k-i\kappa_N)}{(k+i\kappa_{N+1})\times\ldots\times(k+i\kappa_{2N+1})}; \quad \text{(B29)}$$

using the form similar to that in the first part of Eq. (B18), the extremum solution (B26) can be explicitly rewritten as

$$\varphi(x)=2|\omega|\varphi(0)\int\frac{dk}{2\pi}\frac{(k^2+a_1^2)\times\ldots\times(k^2+a_N^2)\cos(kx)}{(k^2+\kappa_{N+1}^2)\times\ldots\times(k^2+\kappa_{2N+1}^2)}. \quad \text{(B30)}$$

2. Expansion around the self-dual solution

To get an approximate expression for $\mathcal{K}(\alpha)$ in a vicinity of $\alpha=\pi/2$, we expand $V_\pm(x,y)$ to first order in $\cos\alpha$, and employ perturbation theory. The solution of the extremum equations at $\alpha_0=\pi/2$ is unique, and the lowest-order nondegenerate perturbation theory suffices. This amounts to evaluating the Euclidean action (17) along the nonperturbed solution $\varphi(x)$, $\vartheta(x)$,

$$\delta\mathcal{S}_q\equiv\frac{T}{4\pi}\sum_n|\omega_n|\,\delta\mathcal{K}_\alpha|\varphi(0)|^2$$

$$=\frac{T}{4\pi}\sum_n\frac{\chi}{2}\int dx\,dy[\overline{\varphi_x'}\,\delta V_+\varphi_y'+\overline{\vartheta_x'}\,\delta V_-\vartheta_y'],$$

where the integration is performed everywhere except the origin, and the potentials

$$\delta V_+=-\frac{xy\cos\alpha}{\sqrt{x^2+y^2}}V'(\sqrt{x^2+y^2}),$$

$$\delta V_-=-\delta V_+\mathrm{sgn}(xy),$$

were found by expanding Eqs. (19), (20).

According to our solution (B27), the functions $\varphi'(x)$, $-\vartheta'(x)\mathrm{sgn}(\omega x)$ are identical, and the two terms give equal contributions, leading to

$$\delta\mathcal{K}_\alpha=-\frac{\chi\cos\alpha}{|\omega||\varphi(0)|^2}\int_{-\infty}^{\infty}dx\,dy\,\overline{\varphi_x'}\varphi_y' y\,\partial_x V(\sqrt{x^2+y^2}).$$

For the Coulomb potential (15), this gives

$$\delta\mathcal{K}_\alpha=\frac{4\chi\cos\alpha}{|\omega|\,|\varphi(0)|^2}\int_0^\infty dx\int_0^\infty dy\frac{xy\,\overline{\varphi_x'}\varphi_y'}{(x^2+y^2+a^2)^{3/2}}.$$

This integral converges at small distances even if we set $a\to 0$; in this scale-invariant limit the ''wave functions'' $\varphi(x)$ can depend only on the dimensionless quantities $|\omega|x$ and χ, $\varphi(x)\equiv\varphi(0)\phi_\chi(|\omega|x)$. Scaling out the frequency leads to a *frequency-independent* correction,

$$\delta\mathcal{K}_\alpha(\omega,\chi)=\chi\mathcal{N}(\chi)\cos\alpha+\mathcal{O}(\chi^2\cos^2\alpha), \quad \omega a\ll 1,$$

$$\mathcal{N}(\chi)\equiv 4\int_0^\infty dx\int_0^\infty dy\,\frac{xy\,\overline{\phi_\chi'}(x)\phi_\chi'(y)}{(x^2+y^2)^{3/2}}. \quad \text{(B31)}$$

This result supports the numerical data, which indicates that $\mathcal{K}_\alpha(\omega)$ is *independent* of ω at small enough frequencies. This statement is true for all finite angles, $|\cos\alpha|<1$, while $\mathcal{K}_{\alpha=0}(\omega)$ diverges logarithmically according to Eq. (22).

The specific value of the correction depends on the coupling constant χ. In the weak-coupling limit, $\chi\ll 1$, the function $\phi_{\chi\to 0}(x)=\exp(-|x|)$, and the integration produces

$$\mathcal{N}(\chi\to 0)\approx 1.51.$$

For finite $\chi>0$, and any given N in the expansion (B28), the explicit form of the integrand in Eq. (B31) can be found with the help of Eq. (B30), and the corresponding value $\mathcal{N}(\chi)$ can be evaluated numerically.

[1] B. I. Halperin, Phys. Rev. B **25**, 2185 (1982).
[2] X.-G. Wen, Phys. Rev. Lett. **64**, 2206 (1990).
[3] X.-G. Wen, Phys. Rev. B **41**, 12 838 (1991).
[4] X.-G. Wen, Phys. Rev. B **43**, 11 025 (1991).
[5] X.-G. Wen, Phys. Rev. B **44**, 5708 (1991).
[6] X.-G. Wen, Int. J. Mod. Phys. B **6**, 1711 (1992).
[7] C. L. Kane and M. P. A. Fisher, Phys. Rev. B **46**, 7268 (1992); **46**, 15 233 (1992)
[8] U. Weiss, Solid State Commun. **100**, 281 (1996).
[9] P. Fendley, A. W. W. Ludwig, and H. Saleur, Phys. Rev. B **52**, 8934 (1995).
[10] C. L. Kane and M. P. A. Fisher, Phys. Rev. Lett. **72**, 724 (1994).
[11] P. Fendley, A. W. W. Ludwig, and H. Saleur, Phys. Rev. Lett. **75**, 2196 (1995).
[12] For review and extensive reference, see C. L. Kane and M. P. A. Fisher, in *Perspectives in Quantum Hall Effects*, edited by S. D. Sarma and A. Pinczuk (Wiley, New York, 1997).
[13] F. P. Milliken, C. P. Umbach, and R. A. Webb, Solid State Commun. **97**, 309 (1996).
[14] I. J. Maasilta and V. J. Goldman, Phys. Rev. B **55**, 4081 (1997); **57**, R4273 (1998).
[15] P. J. Turley *et al.*, Physica B **249-251**, 410 (1998).
[16] M. Ando, A. Endo, S. Katsumoto, and Y. Iye, Physica B **249-251**, 426 (1998).
[17] D. C. Glattli *et al.*, Physica E (Amsterdam) **6**, 22 (2000).
[18] A. H. MacDonald, S. R. E. Yang, and M. D. Johnson, Aust. J. Phys. **46**, 345 (1993); I. L. Aleiner and L. I. Glazman, Phys. Rev. Lett. **72**, 2935 (1994); C. de C. Chamon and X. G. Wen, Phys. Rev. B **49**, 8227 (1994); I. L. Aleiner, D. Yue, and L. I. Glazman, Phys. Rev. B **51**, 13 467 (1995); S. Conti and G. Vignale, *ibid.* **54**, R14 309 (1996).
[19] A. M. Chang, L. N. Pfeiffer, and K. W. West, Phys. Rev. Lett. **77**, 2538 (1996).
[20] M. Grayson *et al.*, Phys. Rev. Lett. **80**, 1062 (1998).
[21] A. H. Castro Neto, C. de C. Chamon, and C. Nayak, Phys. Rev. Lett. **79**, 4629 (1997); J. H. Han and D. J. Thouless, Phys. Rev. B **55**, R1926 (1997); A. V. Shytov, L. S. Levitov, and B. I. Halperin, Phys. Rev. Lett. **80**, 141 (1998); D. V. Khveshchenko, cond-mat/9710137 (unpublished); S. Conti and G. Vignale, J. Phys.: Condens. Matter **10**, L779 (1998); U. Züelicke and A. H. MacDonald, Phys. Rev. B **60**, 1837 (1999); D.-H. Lee and X.-G. Wen, cond-mat/9909160 (unpublished).
[22] U. Züelicke and A. H. MacDonald, Phys. Rev. B **54**, R8349 (1996).
[23] K. Moon and S. M. Girvin, Phys. Rev. B **54**, 4448 (1996).
[24] Y. Oreg and A. M. Finkel'stein, Phys. Rev. B **54**, R14 265 (1996).
[25] K.-I. Imura and N. Nagaosa, Solid State Commun. **103**, 663 (1997).
[26] See, for example, V. J. Emery, in *Highly Conducting One-Dimensional Solids*, edited by J. T. Devreese, R. P. Evrard, and V. E. van Doren (Plenum Press, New York, 1979), p. 247.
[27] The issues of zero-mode quantization are easily resolved in the Hamiltonian formalism. In particular, it was used in a similar problem by Y. Oreg and A. M. Finkel'stein, Phys. Rev. Lett. **74**, 3668 (1995). However, with nonlocal interactions in complicated geometries, we find it more convenient to use the path integral formalism.
[28] L. P. Pryadko and K. Chaltikian, Phys. Rev. Lett. **80**, 584 (1998).
[29] As a result, the zero-mode quantization is identical to that in the Hamiltonian formalism. Thus, the action (2) produces the same finite-size correlation functions as obtained previously, e.g., by V. L. Pokrovsky and L. P. Pryadko, Phys. Rev. Lett. **72**, 124 (1994); M. R. Geller and D. Loss, Phys. Rev. B **56**, 9692 (1997).
[30] H. Yi and C. L. Kane, Phys. Rev. B **53**, 12 956 (1996).
[31] J. K. Jain and S. Kivelson, Phys. Rev. B **37**, 4111 (1988).
[32] A. Schmid, Phys. Rev. Lett. **51**, 1506 (1983).
[33] F. Guinea, V. Hakim, and A. Muramatsu, Phys. Rev. Lett. **54**, 263 (1985).
[34] C. de C. Chamon and E. Fradkin, Phys. Rev. B **56**, 2012 (1997).
[35] V. A. Volkov and S. A. Mikhailov, Zh. Exp. Teor. Fiz. **94**, 217 (1988) [Sov. Phys. JETP **67**, 1639 (1988)].
[36] N. P. Sandler, C. de C. Chamon, and E. Fradkin, Phys. Rev. B **59**, 12 521 (1999).
[37] R. C. Ashoori, H. L. Stormer, L. N. Pfeiffer, K. W. Baldwin, and K. West, Phys. Rev. B **45**, 3894 (1992).
[38] B. Noble, *Methods Based on the Wiener-Hopf Technique for the Solutions of the Partial Differential Equations* (Pergamon, New York, 1958).